Proton Transfer Reaction Mass Spectrometry and the Unambiguous Real-Time Detection of 2,4,6 Trinitrotoluene

ARTICLE *in* ANALYTICAL CHEMISTRY · APRIL 2012

Impact Factor: 5.64 · DOI: 10.1021/ac3004456 · Source: PubMed

9 AUTHORS, INCLUDING:

Kurt Becker
NYU Polytechnic School of Engineering
408 PUBLICATIONS **4,545** CITATIONS
SEE PROFILE

Simone Jürschik
Ionicon Analytik GmbH
19 PUBLICATIONS **198** CITATIONS
SEE PROFILE

Tilmann D Märk
University of Innsbruck
821 PUBLICATIONS **14,627** CITATIONS
SEE PROFILE

Chris Mayhew
Indian Institute of Technology Roorkee
63 PUBLICATIONS **818** CITATIONS
SEE PROFILE

Proton Transfer Reaction Mass Spectrometry and the unambiguous real-time detection of 2,4,6 TNT

Journal:	*Analytical Chemistry*
Manuscript ID:	ac-2012-004456
Manuscript Type:	Article
Date Submitted by the Author:	15-Feb-2012

Complete List of Authors:	Sulzer, Philipp; 1. Ionicon Analytik Gesellschaft m.b.H., Petersson, Fredrick; 2. Institut für Ionenphysik und Angewandte Physik, Argawal, Bishu; 2. Institut für Ionenphysik und Angewandte Physik, becker, Kurt; 3. Polytechnic Institute of New York University, Jürschik, Simone; Ionicon Analytik GmbH, Märk, Tilmann; Leopold Franzens Universit&#65533;t, Institut fuer Ionenphysik und Angewandte Physik Perry, David; School of Physics and Astronomy, Watts, Peter; School of Physics and Astronomy, Mayhew, Chris; University of Birmingham, School of Physics and Astronomy

Proton Transfer Reaction Mass Spectrometry and the unambiguous real-time detection of 2,4,6 TNT

Philipp Sulzer[1], Fredrik Petersson,[1] Bishu Agarwal,[2] Kurt H. Becker,[3] Simone Jürschik,[1] Tilmann D. Märk,[1,2] David Perry,[4] Peter Watts,[4] and Chris A. Mayhew[4*]

1. Ionicon Analytik Gesellschaft m.b.H., Eduard-Bodem-Gasse 3, A-6020 Innsbruck, Austria
2. Institut für Ionenphysik und Angewandte Physik, Leopold Franzens Universität Innsbruck, Technikerstr. 25, A-6020 Innsbruck, Austria
3. Polytechnic Institute of New York University, NY 11201, USA
4. School of Physics and Astronomy, University of Birmingham, Edgbaston, Birmingham, B15 4TT, UK

Abstract

Fears of terrorist attacks have led to the development of various technologies for the real-time detection of explosives, but all suffer from potential ambiguities in the assignment of threat agents. Using proton transfer reaction mass spectrometry an unusual bias dependence in the detection sensitivity of 2,4,6 trinitrotoluene (TNT) on the reduced electric field has been observed, which we relate to unexpected ion-molecule chemistry based upon comparisons of measurements taken with related nitroaromatic compounds (1,3,5 trinitrobenzene, 1,3 dinitrobenzene, and 2,4 dinitrotoluene) and electronic structure calculations. This dependence provides an easily measurable signature that can be used to provide a rapid highly selective analytical procedure to minimise false positives for the detection of TNT. This has major implications for Homeland Security and, in addition, has the potential of making instrumentation cost effective for use in security areas. This study shows that an understanding of fundamental

ion-molecule chemistry occurring in low-pressure drift tubes is needed to exploit selectivity and sensitivity for analytical purposes.

*To whom correspondence should be addressed. E-mail: c.mayhew@bham.ac.uk

Graphical Abstract: Normalised protonated parent ion signal intensities for (a) 2,4 dinitrotoluene (DNT) and (b) 2,4,6 trinitrotoluene (TNT) as a function of reduced electric field (*E*/*N*). For protonated TNT rather than decreasing signal intensity with increasing *E*/*N* , which is the more usual sensitivity pattern observed in PTR-MS studies, an anomalous behavior is first observed, whereby the signal intensity initially rises with increasing *E*/*N* until at relatively high *E*/*N* values a peak is reached after which the signal intensity demonstrates the more usual behaviour.

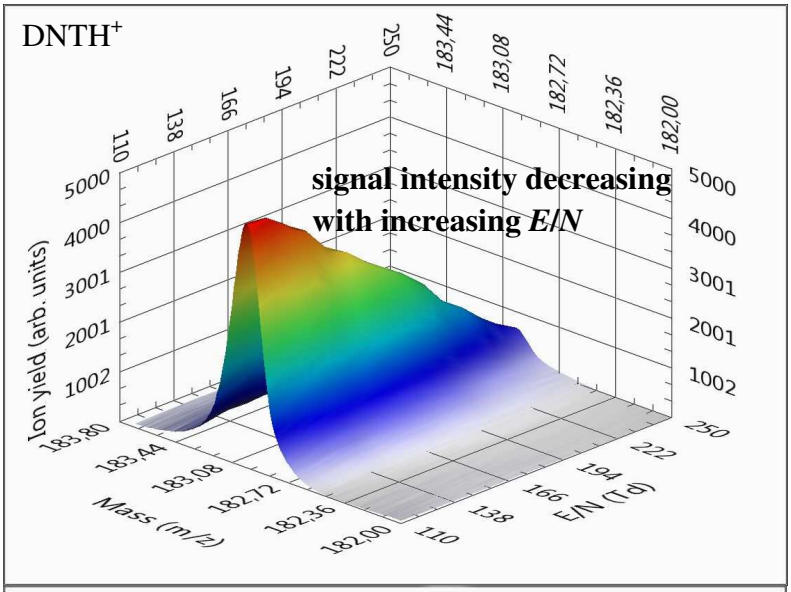
DNTH+
signal intensity decreasing with increasing E/N
Ion yield (arb. units)
Mass (m/z)
E/N (Td)

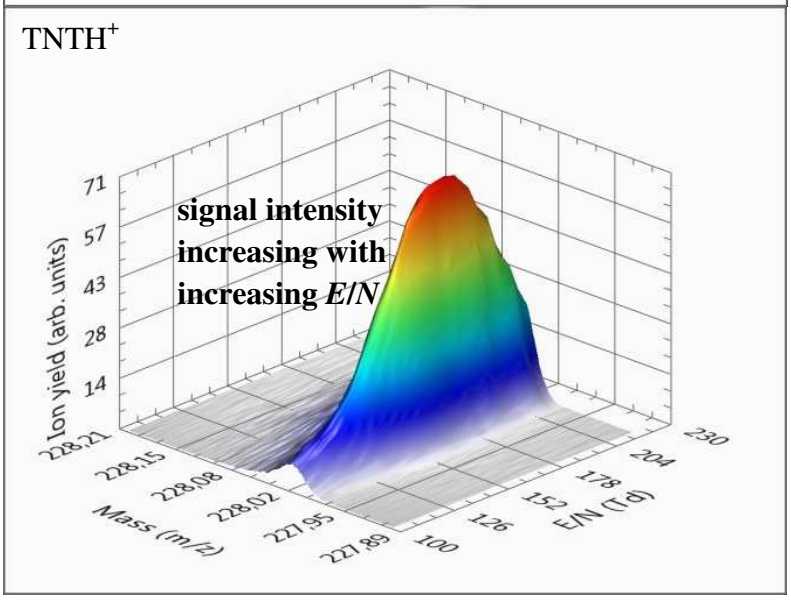
TNTH+
signal intensity increasing with increasing E/N
Ion yield (arb. units)
Mass (m/z)
E/N (Td)

The detection of explosives in real-time and with high sensitivity and selectivity has been an active area of research for many decades.[1,2] Whilst major progress has been made in improving the sensitivity of detection, selectivity is still a problem. The most commonly deployed chemical analysis technology for the detection of explosives is the Ion Mobility Spectrometer (IMS), which is a high pressure (typically one atmosphere) drift tube device incorporating an electric gate to pulse ions into the drift region.[3,4] Despite its sensitivity and robustness, an IMS has limited chemical specificity, partly resulting from its low temporal resolution inherent in the separation of the ion mobility peaks, which can result in false positive signals. Analytical mass spectrometric techniques used in real-world situations for the rapid identification of explosives suffer from the uncertainty of assigning a given m/z in a mass spectrum to a given compound. Consequently, a new approach is needed to detect explosives with high levels of confidence (low rate of false positives) and a sensitivity that equals or surpasses that of an IMS.

Recently, proton transfer reaction mass spectrometry (PTR-MS) has been shown to be a promising analytical platform technology for many areas of science and applications, from fundamental research through to atmospheric pollution and homeland security[5-12] PTR-MS incorporates a drift tube operating at a low pressure (typically 1-2 mbar) as the reaction chamber and a mass spectrometer as an analyser (in this study we have used time-of-flight (ToF) mass spectrometers). H_3O^+ ions are used as the proton donating reagent ion species. Most users of PTR-MS set the drift tube at a fixed reduced electric field (the ratio of the electric field strength E to buffer gas number density N in the drift tube) of between approximately 110-140 Td (1 Td = 10^{-17} V cm^2). This range of values is considered a good compromise between minimal formation of protonated water clusters (predominantly $H_3O^+.H_2O$), limited fragmentation of the protonated parent species and adequate reaction time, thereby maximising the sensitivity for detection of a

compound. If *E*/*N* is increased beyond this value generally the sensitivity for the detection of an analyte is found to decrease with increasing *E*/*N*. This is a result of various instrumental factors, including fragmentation at high *E*/*N* that can result in non-specific product ions, decrease in reaction time (which is proportional to *N*/*E*) and possible *E*/*N* transmission dependences. In contrast to what is normally observed, we found in a proof-of-principle study on the potential use of PTR-MS to detect explosives that for 2,4,6 trinitrotoluene (TNT) the protonated parent signal increased in intensity upon changing *E*/*N* from 90 Td to 140 Td.[9] To investigate this surprising behaviour further and to try to discover its cause, we have undertaken a series of detailed PTR-MS investigations to explore the detection sensitivity for TNT and several related nitroaromatics (2,4 dinitrotoluene (DNT), 1,3,5 trinitrobenzene (TNB) and 1,3 dinitrobenzene (DNB)) over a range of *E*/*N* values, all supported by electronic structure calculations.[13]

The findings of our investigations presented in this paper have major implications for the provision of a real-time analytical mass spectrometric procedure for the detection of TNT with extremely high levels of confidence. Furthermore, these findings open-up future research areas for fundamental studies of ion-molecule reaction processes occurring within the drift tube of a PTR-MS that could be used to exploit selectivity and sensitivity for a broad range of applications (e.g. health and food sciences, atmospheric chemistry and environmental pollution).

Experimental and Theoretical Details

Electronic Structure Calculations

Density Functional Theory calculations using the GAUSSIAN09 PROGRAM with the GaussView 5 interface have been undertaken to determine thermochemical properties of various neutrals, protonated species and reaction processes at 298 K,[13] although it is appreciated that the

drift tube temperature is greater than this, and that of the ions even higher due to the electric field. The B3LYP functional with the 6-31+G(d,p) basis set was used throughout except where otherwise stated. In previous work, a comparison of calculations using both B3LYP and MP2 levels with the 6-311+G(2d,2p) basis set was made.[14] It was found that there were no significant differences in the relative energies for the various species when using either the B3LYP level or the more time-consuming MP2 level. Further work showed no significant differences between results at the B3LYP level using both the 6-31+G(d,p) and 6-311+G(2d,2p) basis sets and thus the lower basis set has been selected for this work as being the most time-efficient. However, in order to have confidence in an unexpected conclusion, some calculations were repeated with the 6-311+G(2d,2p) basis set. The same basis set was used for both the geometry optimisations and frequency calculations, local minima being characterised by the absence of imaginary frequencies. All total energy comparisons include zero point energy corrections. Multiple stable conformations of some species can be found, but as these tend to differ from each other by only a few kJ mol^{-1}, they do not affect the overall reaction coordinate(s) and are thus ignored.

Experimental Methods

PTR-MS is a low-pressure drift tube technology that relies on soft chemical ionisation procedures, whereby the reagent ion H_3O^+ transfers a proton to a chemical species (M) with a proton affinity greater than that of water, and hence the compounds of interest are mass spectrometrically detected usually as MH^+. This makes the identification of a compound in a complex chemical environment easier than using, for example, the more conventional electron impact ionisation mass spectrometry.

Two different Proton Transfer Time-of-Flight Mass Spectrometers (PTR-ToF-MS), one manufactured by Ionicon Analytik GmbH (a PTR-TOF 8000) based in Austria and another manufactured by KORE Technology Ltd based in the UK,[15, 16] were used in this study. The PTR-TOF 8000 was used for TNT and TNB measurements and the KORE PTR-TOF-MS for TNT, DNB and DNT measurements presented in this paper. Full descriptions of the two instruments can be found in previous publications,[17-19] and hence only brief details will be provided here. For both instruments, the H_3O^+ reagent ions are produced from water vapour introduced into a hollow cathode discharge from a liquid water sample holder, either via a mass flow controller (PTR-TOF 8000) or via a needle valve (KORE PTR-ToF-MS). These reagent ions, under the influence of a voltage gradient, pass through a small orifice from the hollow cathode into an adjacent drift tube reaction section, where the sample analyte under investigation is introduced via a gas inlet system. However, it should be appreciated that H_3O^+ is not the only reagent ion present in the drift tube. As a result of clustering, $H_3O^+.nH_2O$ (n =1 and 2) can also be present in the drift tube, the concentrations of which depend on *E*/*N* and humidity. By comparing the ratios of 37 m/z to 19 m/z ion intensities at various *E*/*N* values, we have found that more water vapour from the hollow cathode reaches the drift tube for the KORE instrument than for the PTR-TOF 8000, i.e. the buffer air is more humid in the drift tube of the KORE instrument than found in the Ionicon Analytik GmbH one. This has important consequences for the measurements presented in this paper, which will be described later.

The typical operating drift tube pressures and temperatures used for the measurements presented in this paper were 2.3 mbar and 90 ^oC for the PTR-TOF 8000 and 0.8 mbar and 60 ^oC for the KORE PTR-ToF-MS. The PTR-TOF 8000 has a sensitivity of approximately 50 cps/ppbv at an *E/N* of 140 Td for an H_3O^+ signal intensity of 10^6 cps and a maximum resolution

of 8000 m/Δm. For the KORE PTR-ToF-MS, which is a first generation model, we have determined its sensitivity to be approximately 6 cps/ppbv for an H_3O^+ signal intensity of 10^6 cps at an *E/N* of 140 Td with a maximum resolution of approximately 1000 m/Δm. The actual total H_3O^+ reagent ion signal achievable for the PTR-TOF 8000 and the KORE PTR-TOF-MS is approximately 10^6 cps and 3×10^5 cps, respectively, at *E/N* of 140 Td.

The same measurement procedure was adopted in the two laboratories, namely drawing laboratory air through a hydrocarbon trap into a sealed glass vial, which contained a small quantity of the chemical analyte, maintained at approximately 60 ^oC. This drawn air was passed over the sample and sent to the inlet system. The inlet system was usually maintained at 90 ^oC. The uniform heating of the inlet lines and drift chambers is critical to minimise condensation of the compounds on to the surfaces and thereby improve the explosive concentration in the drift tube. In the case of the PTR-TOF 8000 instrument a long heated inlet line (1 m in length) was used, whereas for the UK measurements we used a much shorter heated inlet system (approximately 10 cm in length). Therefore, although the PTR-TOF 8000 is more sensitive than the KORE PTR-ToF-MS by approximately a factor of 25, higher concentrations of the compounds were present in the drift tube of the KORE instrument than for the PTR-TOF 8000, and this is reflected in the counts per second obtained for the product ions.

TNT was either supplied by the Leopold Franzens Universität Innsbruck for the Austrian measurements or purchased in small quantities (1mg/ml in an AcCN:MeOH (1:1) matrix) from AccuStandard, Inc., for the UK measurements. Before any measurements, the AccuStandard sample was placed in a glass vial and allowed to air-dry. All other chemicals were purchased from Sigma Aldrich.

Normalisation of Data

By varying *E*/*N*, a number of related parameters change which requires consideration in the normalisation of the data produced. These parameters include the total number of reagent ions (in this study H_3O^+ and $H_3O^+.H_2O$), the ratios of H_3O^+ and its hydrates and the reaction time. What cannot be taken into account in the normalisation is the influence of *E*/*N* upon the internal energy of the ions and any concomitant effects upon reaction rates with the neutrals whether they be analyte or water. Furthermore, the observed counts per second (cps) is only a reflection of the number density of ions at the entrance to the mass spectrometer and does not take account of any dependence of the voltages in the drift tube upon the transmission efficiency into the mass spectrometer which in any event is unknown. Nor does it take into account the variations in ion losses due to diffusion and coulombic repulsion of ions to the walls of the drift tube. The ratios of the H_3O^+ and its hydrates will vary as they traverse the drift tube, as the primary source of hydrates is the reaction of H_3O^+ with H_2O in the drift gas. Finally, the reaction time: this obviously varies inversely with *E*/*N* but will also depend upon the mobility of the ion. With such a multiplicity of variables any normalisation must necessarily be empirical and approximate.

To allow for any changes in reagent ion signal as a function of *E*/*N*, we have normalised the data to 10^6 reagent ions per second, because that is the typical ion current obtained using a PTR-TOF 8000 instrument. The normalised intensities shown in the figures that follow in this paper refer to those obtained by integrating over the spectral line (including the spectral line associated with the ^{13}C isotope), dividing by the integrated reagent ion signal and multiply by 10^6. Since MH^+ can only be formed by reaction of M with H_3O^+, all other routes being both endoergic and endoergonic, its ion count is normalised against H_3O^+. However, this approach is not appropriate for normalisation of $MH^+.H_2O$ as this can, if energetically feasible, be formed

directly by a bimolecular reaction of M with $H_3O^+.H_2O$ and indirectly by an association reaction of MH^+ with H_2O. Therefore, the $MH^+.H_2O$ ion signal intensities are normalised to the sum of H_3O^+ and $H_3O^+.H_2O$ reagent ions at each *E*/*N* value. We comment that this is not an ideal procedure at *E*/*N* values where $H_3O^+.H_2O$ is observed in significant amounts (below approximately 140 Td), because we do not know the efficiencies of the reactions and because we are only determining the H_3O^+:$H_3O^+.H_2O$ ratio at the mass spectrometer detector, we do not know what the actual ratio in the drift tube is owing to possible fragmentation of $H_3O^+.H_2O$ at the interface between the drift tube and the spectrometer.

As mentioned above, varying *E*/*N* will also affect the reaction time, which is a linear function of *N*/*E*, and is relatively easy to take this into account. However, this ignores the changes in the mobility of the ion, and given that the protonated parent undergoes a secondary reaction with H_2O at low *E*/*N*, we have not taken into account changes in reaction time.

Results

Electronic structure calculations

Since much of the thermochemistry of the reaction processes involved in this study is unknown, a series of extensive electronic structure calculations have been undertaken.[13] These provide crucial information to determine which reaction pathways are possible. The calculations are summarized in tables 1-3. Table 1 presents the calculated proton affinities and gas phase basicities for TNT, DNT, TNB and DNB. Table 2 presents the changes in the enthalpies and free energies for the reactions of H_3O^+, $H_3O^+.H_2O$ and $H_3O^+.2H_2O$ with TNT, DNT, TNB and DNB. Table 3 provides the changes in the enthalpies and free energies for the reactions of $MH^+.nH_2O$ (M = TNT, DNT, TNB or DNB and n = 0, 1 or 2) with H_2O.

Table 1. Proton affinities (PA) and gas phase basicities (GB) for TNT, DNT, TNB and DNB at 298 K calculated at the B3LYP 6-31+G(d,p) level.

	PA kJ mol^{-1}	GB kJ mol^{-1}
TNT	744	713
DNT	782	751
TNB	722	690
DNB	761	729

Table 2. Enthalpy and free energy changes for the reactions of H_3O^+, $H_3O^+.H_2O$ and $H_3O^+.2H_2O$ with TNT, DNT, TNB and DNB at 298 K calculated at the B3LYP 6-31+G(d,p) level.

Reactant	Product	ΔH_{298} kJ mol^{-1}	ΔG_{298} kJ mol^{-1}
TNT + H_3O^+	$TNTH^+.H_2O$	-161	-128
	$TNTH^+ + H_2O$	-59	-59
TNT + $H_3O^+.H_2O$	$TNTH^+.2H_2O$	-85	-48
	$TNTH^+.H_2O + H_2O$	-3	-5
TNT + $H_3O^+.2H_2O$	$TNTH^+.2H_2O + H_2O$	+10	+16
DNT + H_3O^+	$DNTH^+.H_2O$	-192	-157
	$DNTH^+ + H_2O$	-98	-97
DNT + $H_3O^+.H_2O$	$DNTH^+.2H_2O$	-108	-71
	$DNTH^+.H_2O + H_2O$	-34	-33
DNT + $H_3O^+.2H_2O$	$DNTH^+.2H_2O + H_2O$	-13	-7
TNB + H_3O^+	$TNBH^+.H_2O$	-146	-94
	$TNBH^+ + H_2O$	-38	-21
TNB + $H_3O^+.H_2O$	$TNBH^+.2H_2O$	-75	-38
	$TNBH^+.H_2O + H_2O$	+12	+14
TNB + $H_3O^+.2H_2O$	$TNBH^+.2H_2O + H_2O$	+20	+26
DNB + H_3O^+	$DNBH^+.H_2O$	-177	-141
	$DNBH^+ + H_2O$	-76	-76
DNB + $H_3O^+.H_2O$	$DNBH^+.2H_2O$	-98	-61
	$DNBH^+.H_2O + H_2O$	-19	-17
DNB + $H_3O^+.2H_2O$	$DNBH^+.2H_2O + H_2O$	-3	-4

Table 3. Enthalpy and free energy changes for the reactions of $MH^+.nH_2O$ (M = TNT, DNT, TNB or DNB, and n = 0, 1 or 2) with H_2O at 298 K calculated at the B3LYP 6-31+G(d,p) level.

Reactant	Product	ΔH_{298} kJ mol^{-1}	ΔG_{298} kJ mol^{-1}
$TNTH^+ + H_2O$	$TNTH^+.H_2O$	-102	-69
$TNTH^+.H_2O + H_2O$	$TNTH^+.2H_2O$	-82	-44
	$TNT + H_3O^+.H_2O$	+3	+5
$TNTH^+.2H_2O + H_2O$	$TNTH^+.3H_2O$	-72	-16
	$TNT + H_3O^+.2H_2O$	-10	-16
$DNTH^+ + H_2O$	$DNTH^+.H_2O$	-94	-59
$DNTH^+.H_2O + H_2O$	$DNTH^+.2H_2O$	-74	-38
	$DNT + H_3O^+.H_2O$	+34	+33
$DNTH^+.2H_2O + H_2O$	$DNTH^+.3H_2O$	-69	-38
	$DNT + H_3O^+.2H_2O$	+13	+7
$TNBH^+ + H_2O$	$TNBH^+.H_2O$	-108	-74
$TNBH^+.H_2O + H_2O$	$TNBH^+.2H_2O$	-86	-51
	$TNB + H_3O^+.H_2O$	-12	-14
$TNBH^+.2H_2O + H_2O$	$TNBH^+.3H_2O$	-75	-43
	$TNB + H_3O^+.2H_2O$	-20	-26
$DNBH^+ + H_2O$	$DNBH^+.H_2O$	-100	-65
$DNBH^+.H_2O + H_2O$	$DNBH^+.2H_2O$	-82	-44
	$DNB + H_3O^+.H_2O$	+19	+17
$DNBH^+.2H_2O + H_2O$	$DNBH^+.3H_2O$	-71	-37
	$DNB + H_3O^+.2H_2O$	+3	+4

Proton Transfer Reaction Time-of-Flight Mass Spectrometric Results

Figures 1 (a) and (b) show the detection efficiency for $TNTH^+$ as a function of *E*/*N* using the normalised integrated mass spectral line intensity measured either with a PTR-TOF 8000 or a KORE PTR-ToF-MS, respectively. For figure 1 (b) we have also included the signal intensity associated with the cluster ion $TNTH^+.H_2O$, for reasons that will be discussed later. Note that the normalised counts per second (ncps) shown on the figures are a reflection of both the sensitivity of the instruments (which is greater for the PTR-TOF 8000) and the concentrations of the explosive present in the drift tube. Therefore, the absolute values of the intensities are not important, rather it is the dependence of the intensity on the *E*/*N* values. From these figures it can be seen that at 140 Td, which was the maximum value used in our proof-of-principle investigation,[9] the sensitivity for $TNTH^+$ detection using PTR-MS has not reached its maximum value. This is only reached at higher *E*/*N*. Whilst the results from the two instruments show a similar trend, which serves to demonstrate that the cause is not an instrumental artefact, there is a difference at which *E*/*N* value the peak value in the $TNTH^+$ intensity is obtained. This provides a clue as to what may be occurring, as will be explained later.

Following the unexpected measurements with TNT, we undertook a series of measurements on related compounds, namely TNB, DNT and DNB, in order to determine whether the behaviour occurs for other nitroaromatics and to provide further experimental data to hopefully explain the TNT results. We found that the behaviour displayed for $TNTH^+$ is mirrored by that of $TNBH^+$, as shown in figure 2 using data recorded using the PTR-TOF 8000 (similar results were obtained with the KORE instrument). The results for DNT and DNB, recorded using the KORE instrument, are presented in figures 3 (a) and (b), respectively. In comparison to the TNT and TNB measurements, for DNT and DNB significant intensities of

Figure 1. The variation in normalised integrated signal intensities for protonated TNT as a function of *E*/*N* measured using (a) a PTR-TOF 8000 and (b) a KORE Ltd. PTR-ToF-MS. For figure 1 (b) the signal intensity for $TNTH^+.H_2O$ is also included to illustrate the low signal intensity associated with that ion. Given that similar results were obtained on two different instruments, we can rule out instrumental causes to the unusual behaviour.

(a)

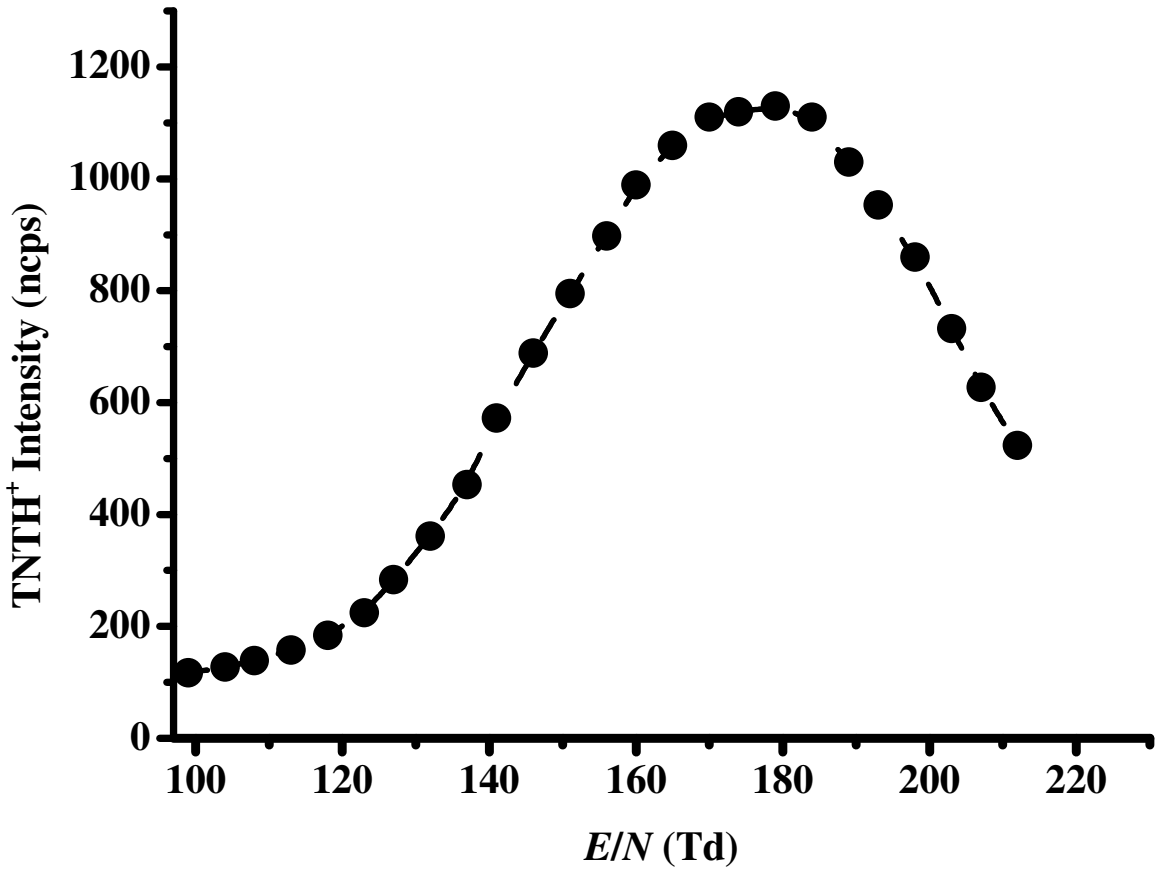

(b)

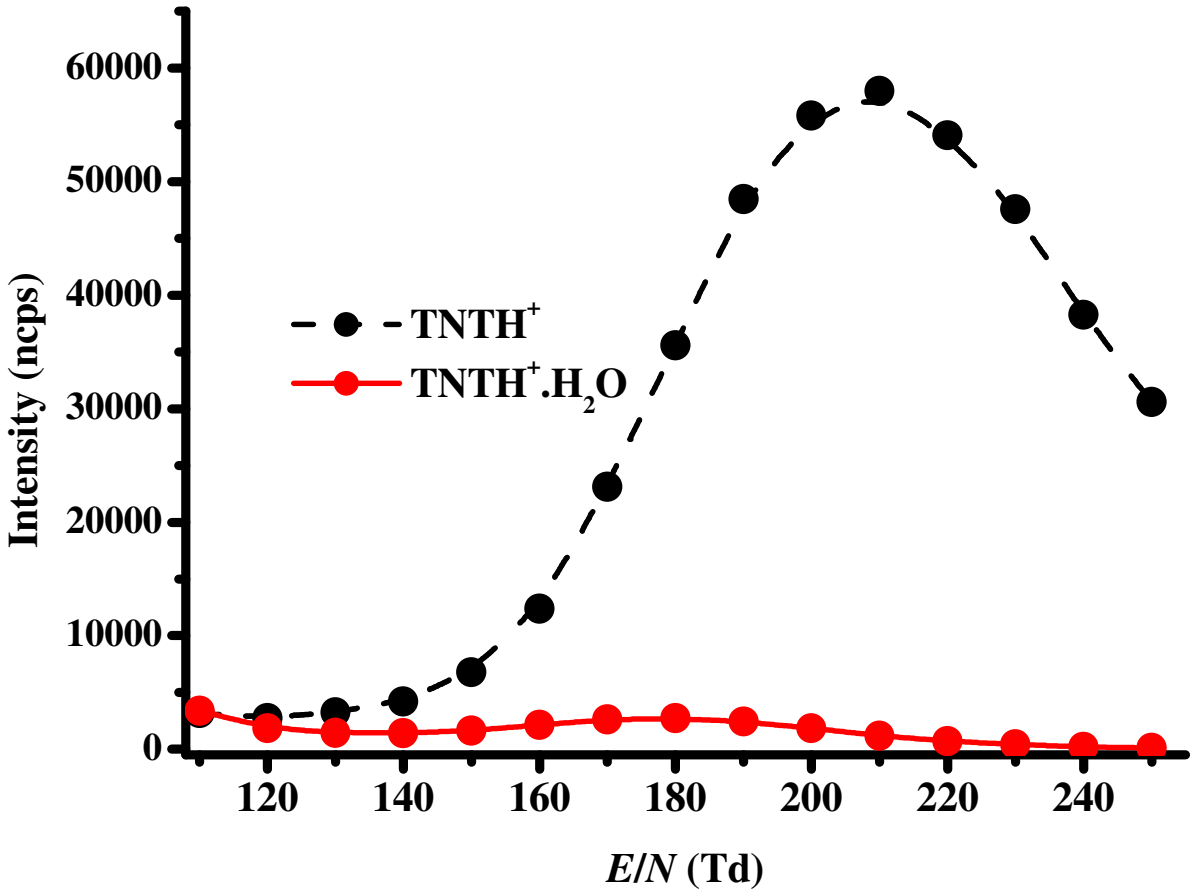
60000
50000
40000
30000
20000
10000
0
Intensity (ncps)
TNTH+
TNTH+.H2O
120
140
160
180
200
220
240
E/N (Td)

Figure 2. The variation in normalised signal intensities for protonated TNB as a function of *E*/*N* recorded on a PTR-TOF 8000.

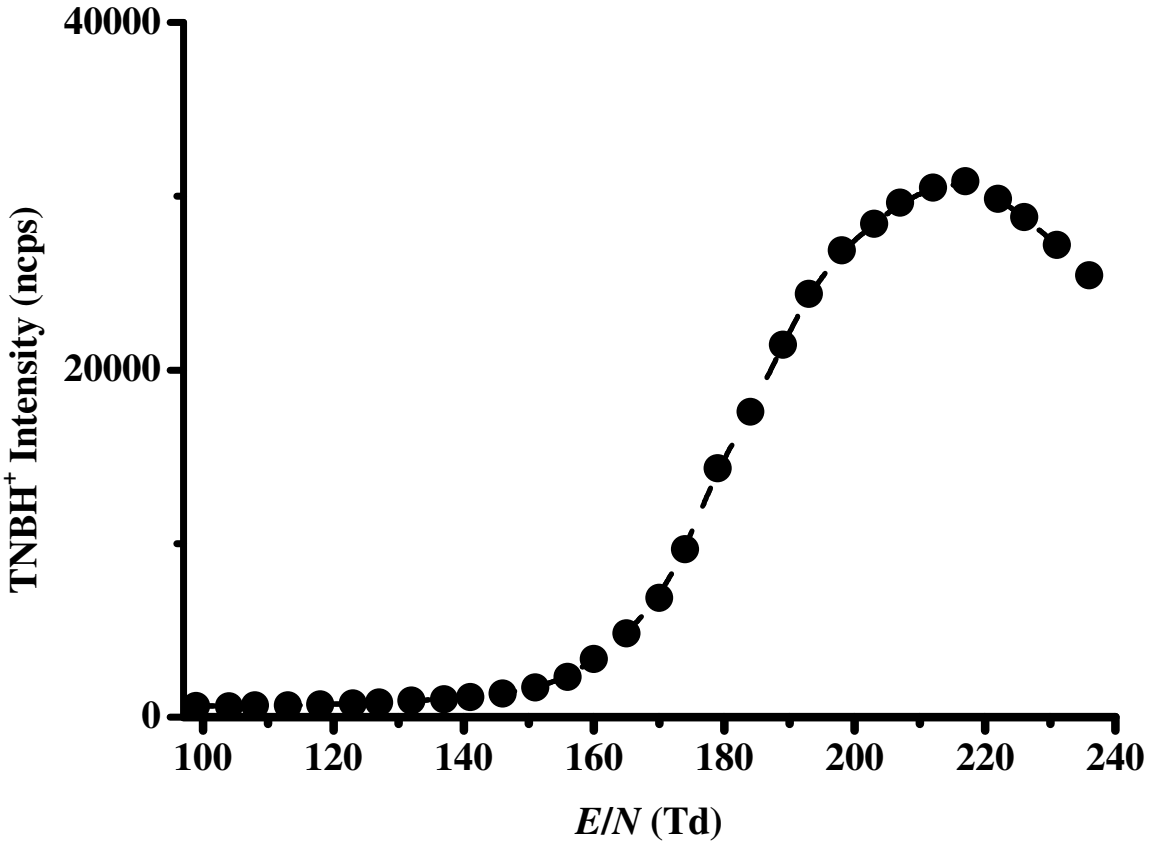

Figure 3. Sensitivity for detection of (a) DNT and (b) DNB as a function of *E*/*N* recorded on a KORE PTR-ToF-MS. Shown are the normalised integrated protonated parent and protonated parent water clusters signals and the sum of these signals. These figures show that the sensitivity for detection of these two compounds (defined as the sum of those product ions that contain the parent neutral) decreases with increasing *E*/*N*. The difference in the variation in the sum of the product ions as a function of *E*/*N* between DNT and DNB is attributed to differences in the efficiencies of the reactions leading to $MH^+.H_2O$ ions.

(a)

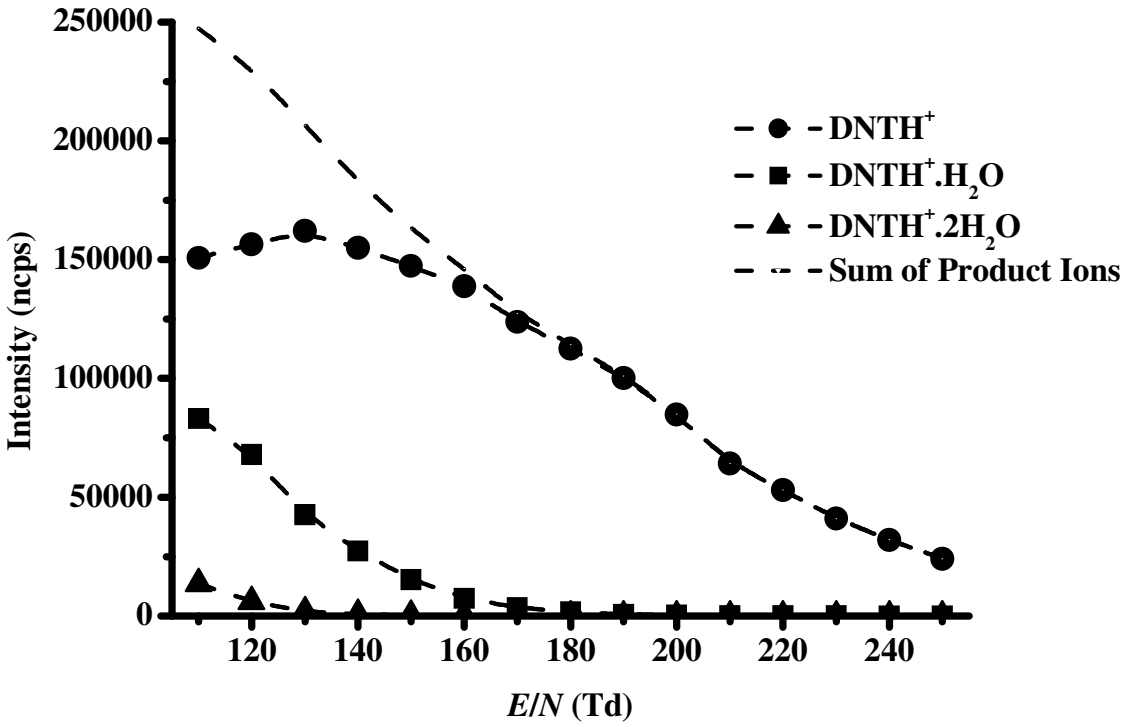

(b)

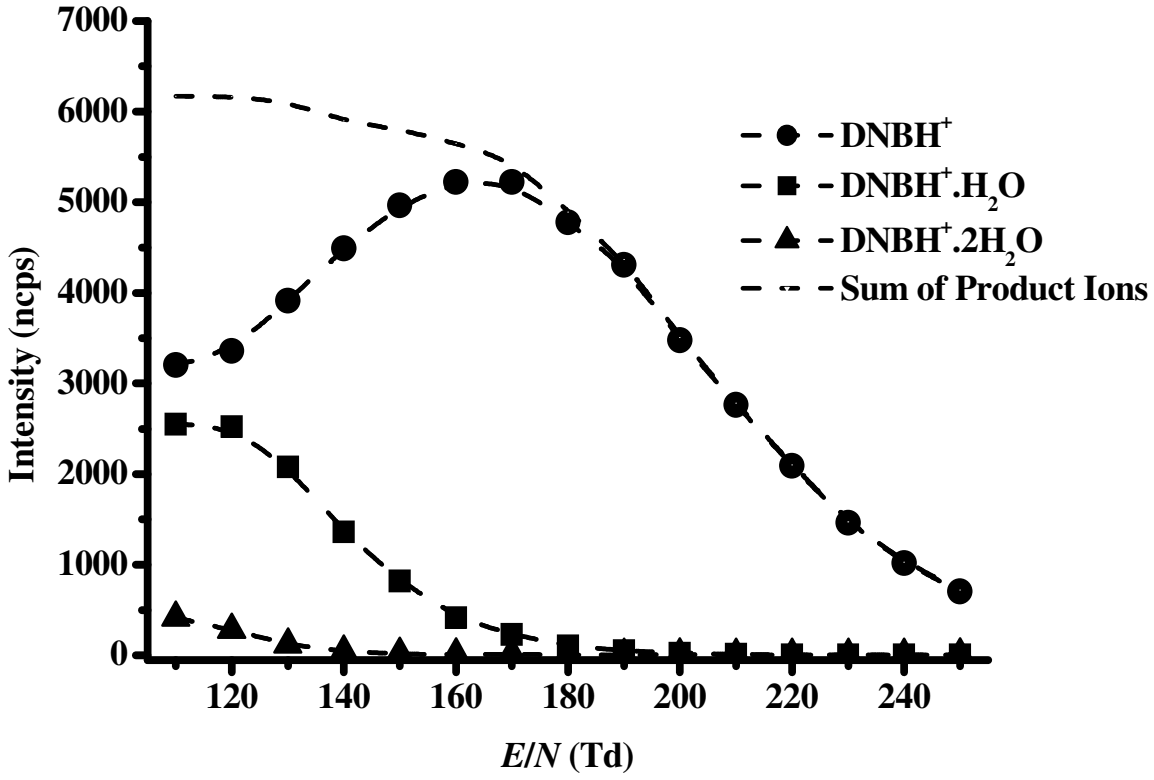
7000
6000
5000
4000
3000
2000
1000
0
Intensity (ncps)
120
140
160
180
200
220
240
E/N (Td)
DNBH+
DNBH+.H2O
DNBH+.2H2O
Sum of Product Ions

MH+.nH_2O (n = 1 and 2) were observed at low *E*/*N*. Therefore, figures 3 (a) and (b) provide signal intensities for all those product ions that are found to incorporate the parent molecules (DNT and DNB), namely the protonated parent (MH^+) and the adduct of the protonated parent with neutral waters.

Discussion

The interpretation of the DNT and DNB results shown in figure 3 is relatively straightforward. The protonated parent ions, MH^+, are produced by a bimolecular proton transfer reaction of the neutral with H_3O^+. The monohydrates, $MH^+.H_2O$, can either be formed by a bimolecular reaction with $H_3O^+.H_2O$ or by an association reaction of MH^+ with H_2O (see thermodynamic calculations in Tables 2 and 3). Whilst formation of the dihydrates, $MH^+.2H_2O$, is just thermodynamically feasible by reaction of M with $H_3O^+.2H_2O$, no significant quantities of $H_3O^+.2H_2O$ are observed and thus formation of the dihydrate is attributed to an association reaction of $MH^+.H_2O$ with H_2O. The association of the protonated parent with waters leads to the observed reduction in its signal intensity at the low *E*/*N* values. However, overall figure 3 shows that the detection sensitivity for DNT and DNB, which we define to be the sum of the product ions that contain the parent neutral molecule, decreases with *E*/*N*, i.e. as often observed in PTR-MS measurements, the detection sensitivity for a compound decreases with increasing *E*/*N*.

The rapid fall-off at low *E*/*N* of the $TNTH^+$ and $TNBH^+$ signals (figures 1 and 2), which is particularly pronounced for TNB, can not immediately be attributed to formation of hydrates, although these are thermodynamically stable (see Tables 2 and 3), because there are only insignificant ion intensities detected for water adducts with $TNTH^+$ and $TNBH^+$ (as illustrated in

figure 1 (b) for TNT). This puzzle can be explained by considering the type of reaction processes that can occur in the drift tube of a PTR-MS when using water ion-chemistry.

In principle, for any $MH^+.nH_2O$ where n = 0, 1, or 2, two reactions with water are possible. One is to form a higher hydrate and the other is to revert to M and a protonated water species. The results of the electronic structure calculations for these two processes for the various M are given in Table 3 and are summarised schematically in figures 4 (a) and (b) for $MH^+.H_2O$ and $MH^+.2H_2O$ reactions, respectively. Because some of the ΔHs and ΔGs are small, calculations on some systems were repeated at the higher basis set with the results shown in square brackets [ ] on the figure. No appreciable differences were found. In interpreting figures 4 (a) and (b), it is important to note that equilibrium is far from being attained in the PTR-MS and that observed ion intensities will be kinetically rather than thermodynamically controlled. Thus, although formation of higher hydrates is always the most thermodynamically favoured process, it requires collisional stabilisation to result in a stable ion whereas dissociation (if thermodynamically allowed) following addition of water to give M and a protonated water cluster can occur directly and, even if slightly endergonic, effectively irreversibly. Consider $DNTH^+.H_2O$ and $DNBH^+.H_2O$ in Figure 4 (a). Reaction of $MH^+.H_2O$ with H_2O to form a higher hydrate is, energetically, considerably more favourable than the endergonic dissociation to M and $H_3O^+.H_2O$. Thus, at *E*/*N* values for which protonated DNT and DNB can efficiently associate with neutral water the protonated parent ion signal intensity will decrease, but a product ion is still observed containing the original analyte. In contrast to $DNTH^+.H_2O$ and $DNBH^+.H_2O$, for $TNBH^+.H_2O$ both formation of the higher hydrate and dissociation to TNB and $H_3O^+.H_2O$ are favourable, but the bimolecular pathway will dominate over the three body association pathway, and given that the back reaction following dissociation is endoergonic, i.e.

Figure 4. Graphical representation of the electronic structure calculations for changes in free energies (in units of kJ mol^{-1}) for the reactions of (a) $MH^+.H_2O$ and (b) $MH^+.2H_2O$ with H_2O using the values provided in table 3. ΔG values calculated using B3LYP functional with the 6-31+G(d,p) basis set are shown in ( ). As some of the ΔGs are small, calculations on some systems were repeated at the higher basis set (6-311+G(2d,2p)) with the results shown in [ ] in the figures.

(a)

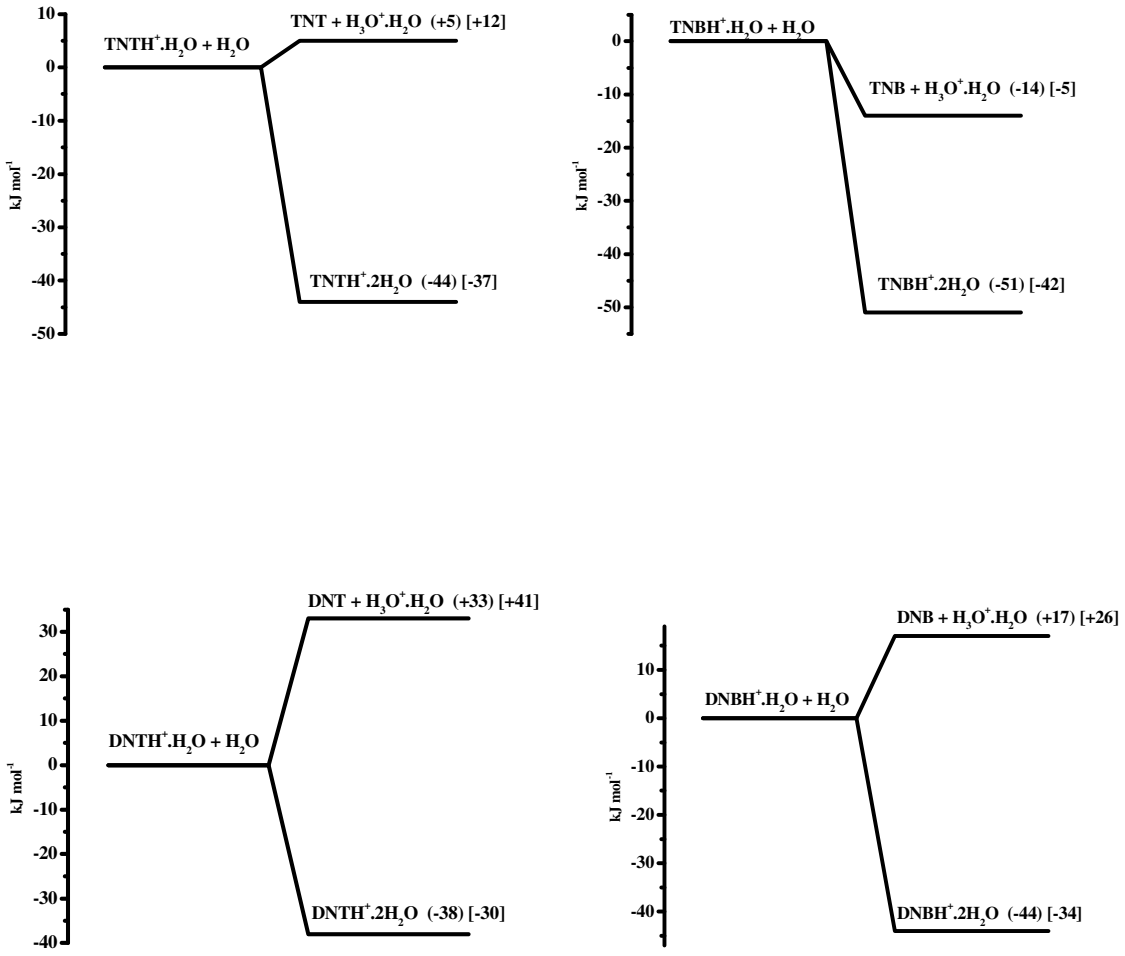

(b)

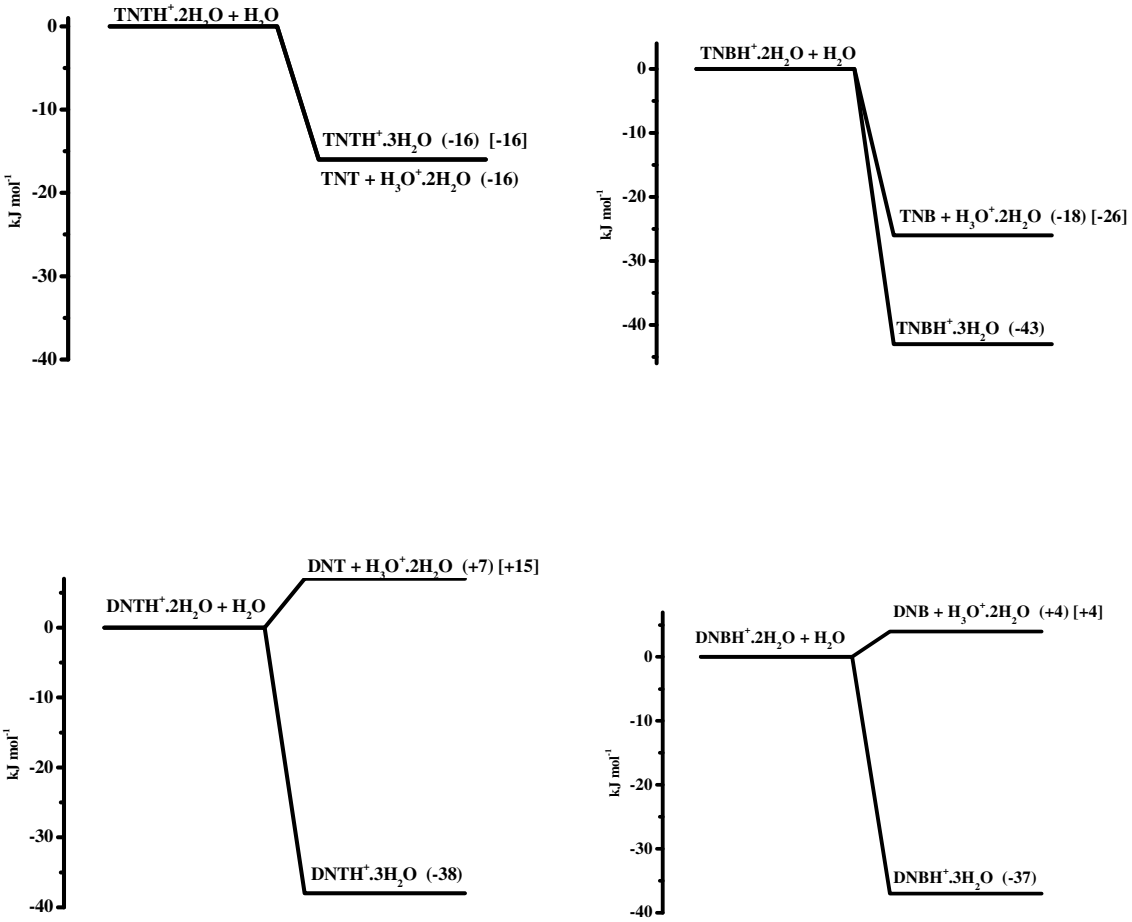
TNTH+.2H2O + H2O
TNTH+.3H2O (-16) [-16]
TNT + H3O+.2H2O (-16)
TNBH+.2H2O + H2O
TNB + H3O+.2H2O (-18) [-26]
TNBH+.3H2O (-43)
DNTH+.2H2O + H2O
DNT + H3O+.2H2O (+7) [+15]
DNTH+.3H2O (-38)
DNBH+.2H2O + H2O
DNB + H3O+.2H2O (+4) [+4]
DNBH+.3H2O (-37)
kJ mol-1
0
-10
-20
-30
-40

effectively irreversible, the final product ion does not contain TNB, but an ion that cannot be detected above the signal intensity associated with the reagent ion $H_3O^+.H_2O$ at 37 m/z, which is always present with a high signal intensity at low *E*/*N*. TNT provides a less clear-cut case as, following association of $TNTH^+.H_2O$ with H_2O, the dissociation pathway is slightly endoergonic although kinetically driven by the high water number density. This small endergonicity results in a slower dissociation than that occurring with TNB and is consistent with the shallower fall-off at low *E*/*N* observed for TNT compared to that of TNB. Thus overall for TNT and TNB at *E*/*N* values whereby protonated parent water adducts are formed, they are lost via a sequential reaction pathway:

$$MH^+.H_2O + H_2O \rightarrow H_3O^+.H_2O + M \qquad (1)$$

where M = TNT or TNB, resulting in a product ion that does not contain the explosive. Furthermore, even if three body association reaction pathway does occur, the bimolecular reaction pathway:

$$MH^+.2H_2O + H_2O \rightarrow H_3O^+.2H_2O + M \qquad (2)$$

is facile for both TNT and TNB with ΔG = -16 kJ mol^{-1} and -26 kJ mol^{-1}, respectively. In comparison, only formation of higher hydrates is thermodynamically allowed for $DNTH^+$ and $DNBH^+$. Regression to DNT and DNB and protonated water clusters is unfavourable. To summarise, the cause for the lack of $MH^+.n(H_2O)$ signals with any significant intensities for M = TNT or TNB is a result of their rapid reactions with H_2O leading to the production of

$H_3O^+.nH_2O$ ions, and this in turn leads to the observed reduction in the sensitivity of detection of TNT and TNB at low *E*/*N*. That a plateau in the normalised protonated parent ion signals is not reached as *E*/*N* increases is a result of the various instrumental factors mentioned earlier such as reduced reaction time, fragmentation at high *E*/*N*, and *E*/*N* transmission dependences, leading ultimately to a reduction in sensitivity.

If the proposed water ion-molecule reaction scheme for TNT and TNB is correct, then the detection sensitivity for TNT and TNB will be dependent on the humidity of the air present in the drift tube of the PTR-MS, which in turn is dependent on the humidity of the inlet air and the amount of neutral water entering the drift tube from the ion source. The production of $MH^+.H_2O$ (M = TNT or TNB) and its reaction with water will increase as the humidity is increased, which will rapidly result in the production of $H_3O^+.H_2O + M$. We can therefore predict a number of changes to the sensitivity of detection of $TNTH^+$ and $TNBH^+$ with increasing humidity. For examples, we can predict that (i) for a fixed *E*/*N*, at or below the peak intensity, the sensitivity for detection of MH^+ should decrease with increasing humidity and (ii) the position of the peak intensity will shift to higher *E*/*N* as the humidity is increased. Therefore, using a PTR-TOF 8000 we measured the effect of inlet humidity on the $TNTH^+$ intensity for fixed *E*/*N* (at approximately 180 Td) and on the *E*/*N* value of the peak position. These measurements for TNT are presented in figure 5, the results of which follow the predicted dependences (identical dependences were found for TNB). This humidity dependence also explains the observed differences in the peak positions for the two instruments. In comparison to the PTR-TOF 8000, more water vapour enters the drift tube from the ion source in the KORE instrument (as determined by the ratio of 37 m/z to 19 m/z for a given *E*/*N*) resulting in a more humid environment, which acts to shift the peak intensity of the $TNTH^+$ signal to higher *E*/*N*, as observed (figure 1 (a) compared to figure 1

Figure 5. Effect of inlet humidity (a) on the detection sensitivity of $TNTH^+$ at a fixed *E*/*N* of approximately 180 Td and (b) on the *E*/*N* value for the position of the peak $TNTH^+$ intensity, measured using a PTR-TOF 8000.

(a)

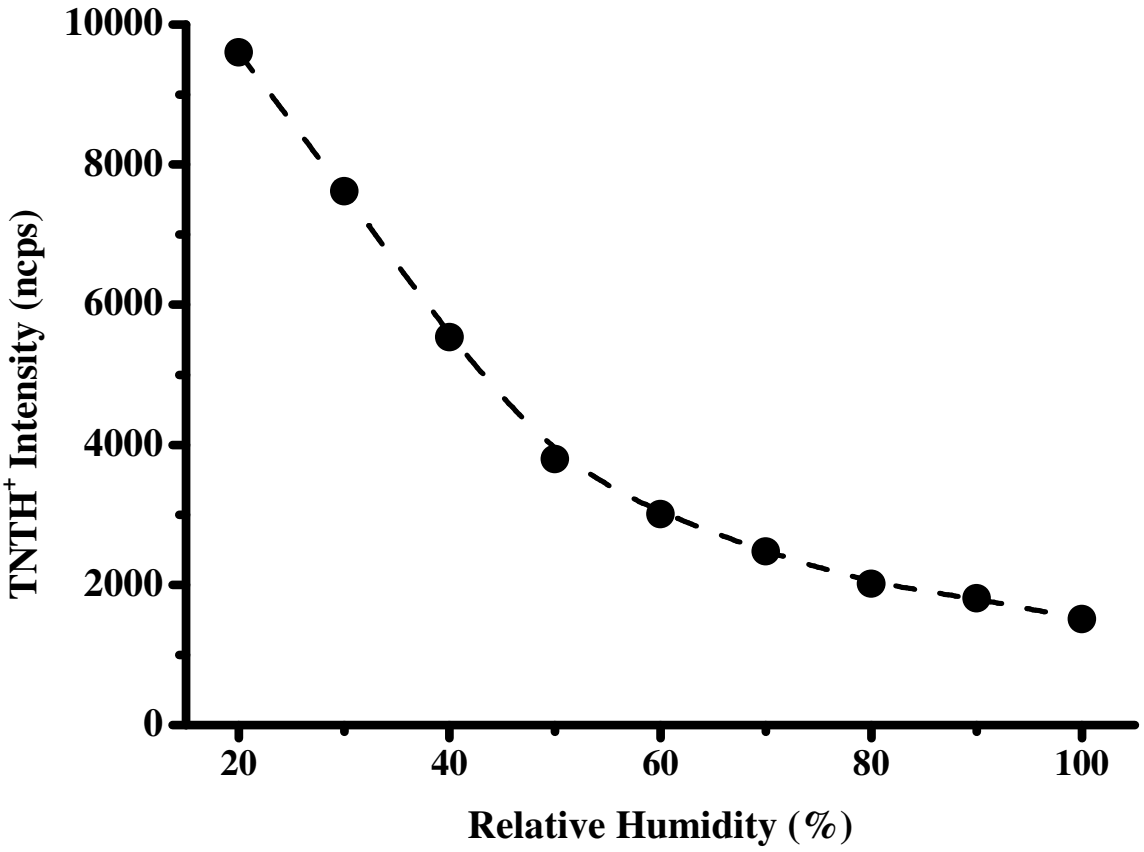

(b)

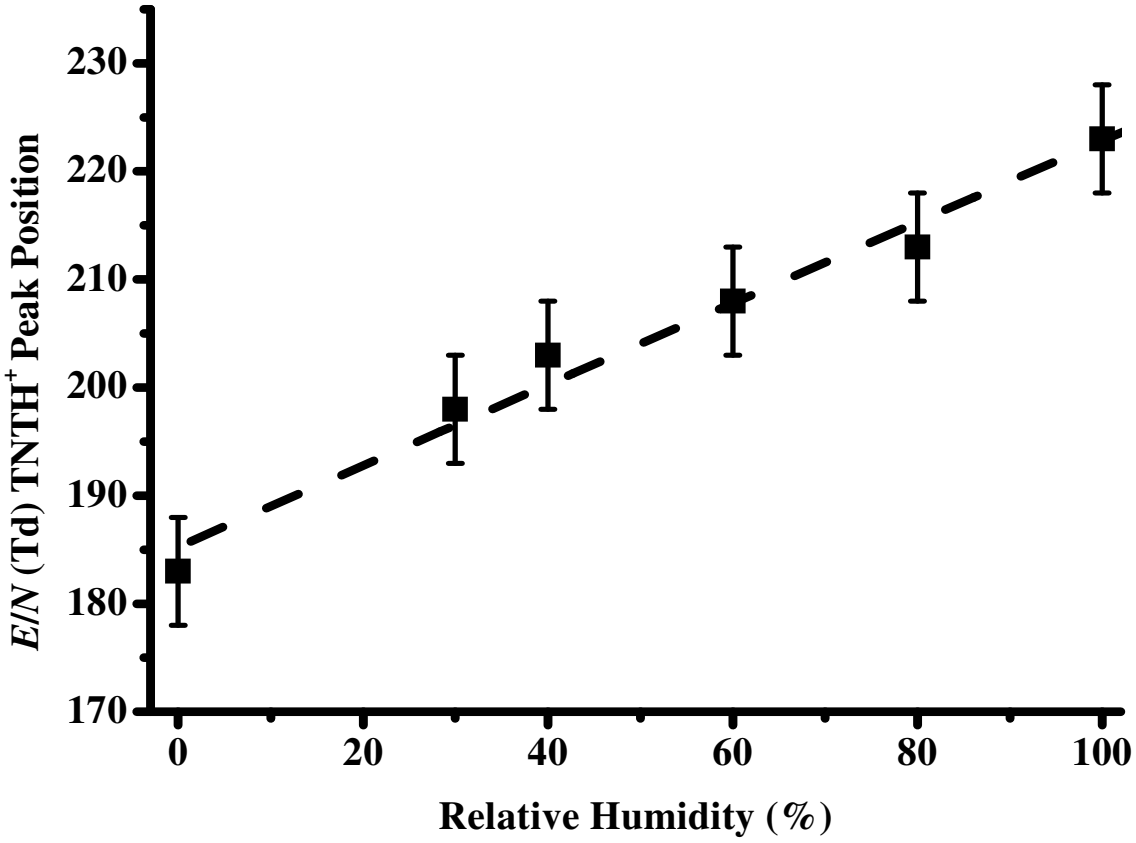
E/N (Td) TNTH+ Peak Position
230
220
210
200
190
180
170
0
20
40
60
80
100
Relative Humidity (%)

(b)). These humidity measurements therefore provide confirmatory results supporting our proposed ion-molecule reaction scheme for TNT and TNB. It is important to note that it is impossible to eliminate completely water in the drift tube when running PTR-MS with H_3O^+ as the dominant reagent ion owing to water vapour entering the drift tube from the ionisation source. However, by running the ionisation source in oxygen we have found that there is sufficient residual water vapour to provide an H_3O^+ signal of sufficient intensity to investigate the reactions of H_3O^+ with TNT. If in addition to this, the inlet air is passed through a moisture trap before being introduced into the drift tube, the humidity in the drift tube can be significantly reduced – essentially resulting in a "dry" system. Under these circumstances, if the proposed reaction model is correct then the $TNTH^+$ signal intensity should follow the more usual behaviour of decreasing intensity with increasing *E*/*N*. These measurements are presented in figure 6 recorded using a KORE PTR-ToF-MS, and which do in fact show this expected behaviour, thereby providing the most convincing evidence that the proposed reaction process occurring in a "wet" drift tube system is correct. Of course when operating the ionisation source with O_2, the major reagent ion is not H_3O^+ but O_2^+, and we find that O_2^+ reacts with TNT predominantly via dissociative charge transfer to produce an ion at 210 m/z as the dominant product, which corresponds to a loss of a hydroxyl radical, i.e.

$$O_2^+ + TNT \rightarrow [TNT - OH]^+ + OH + O_2 \ .$$

This is not the first reported case of humidity effects on the sensitivity of detection of the protonated parent using PTR-MS. There have been a number of studies involving the reactions of protonated formaldehyde and hydrogen cyanide with water,[20-25] which demonstrate that the reverse reaction reduces the sensitivity of detection of these compounds, owing to their proton affinities being close to that of H_2O, and therefore the greater the humidity the greater the

Figure 6. The detection sensitivity for TNT monitoring the $TNTH^+$ and $TNTH^+.H_2O$ signals as a function of *E*/*N* using a "dry" drift tube. Within this dry chemical environment the $TNTH^+$ signal shows the more usual dependence of decreasing sensitivity with increasing *E*/*N*.

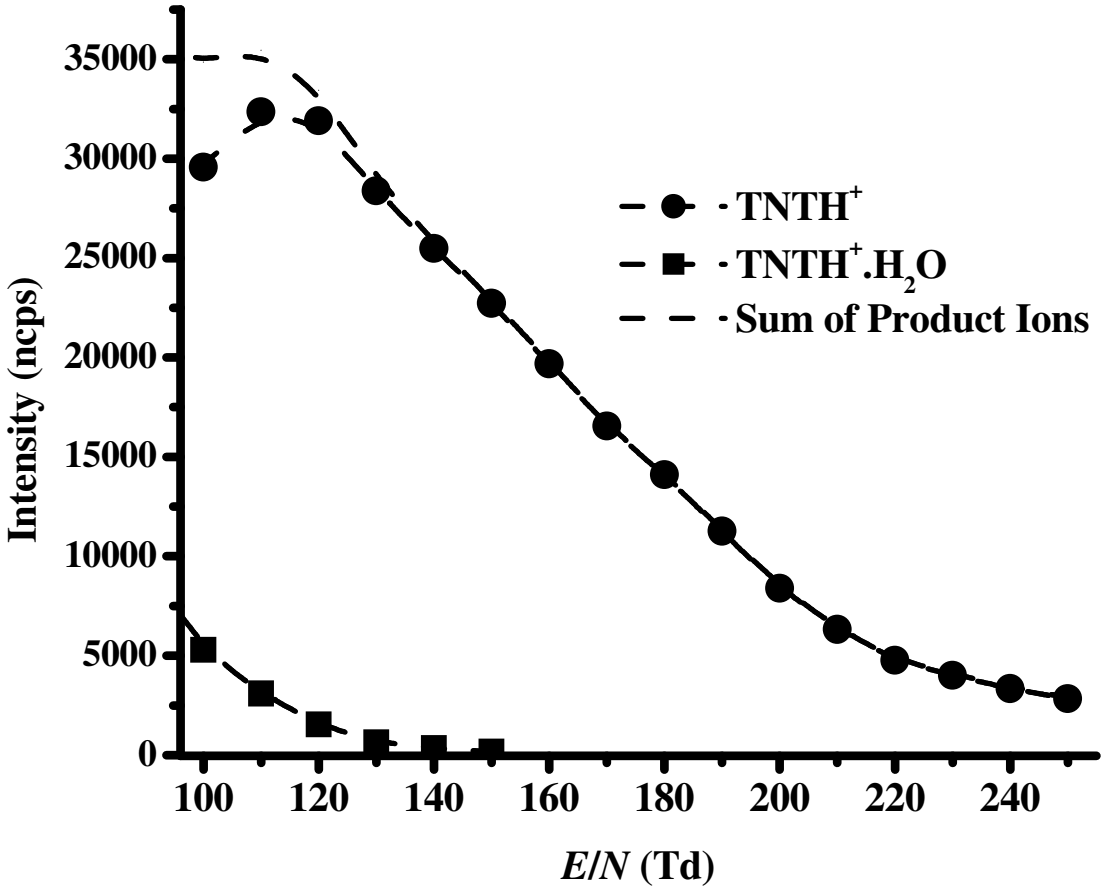

reduction in sensitivity. However, to our knowledge this present study is the first reported case of humidity effects on the sensitivity of detection by PTR-MS techniques involving the hydrated protonated parent ($MH^+.H_2O$) in a bimolecular ion-molecule process with H_2O.

Conclusions

In summary, the difference in behaviour of the protonated parent ion signal intensities observed between the nitroaromatic compounds can be explained either by the occurrence of (for TNT and TNB) or a lack of (for DNT and DNB) secondary bimolecular reactions of $MH^+.H_2O$ with water. At an appropriate *E*/*N* within the drift tube, $TNTH^+$ and $TNBH^+$ can associate with water to form $TNTH^+.n(H_2O)$ and $TNBH^+.n(H_2O)$ ions (n = 1 and 2), respectively. However, once formed, a sequential rapid bimolecular reaction with water leads to $H_3O^+.nH_2O$ as the product ions. The rate of production of the protonated water clusters are strongly favoured owing to the thermochemistry and the far greater concentration of water in the drift tube compared to that of TNT and TNB, and therefore the corresponding protonated parent signal shows a significant drop in intensity as *E*/*N* is reduced below the peak value for a given humidity.

Although chemically interesting in their own right, from an analytical perspective the results presented in this paper have two important practical implications for the detection of TNT when using PTR-MS. The first is that the drift tube of a PTR-MS must be set at an appropriate *E*/*N* value in order to maximize the sensitivity of detection. In particular, operating at standard *E*/*N* values of 110 - 140 Td (as recommended by manufacturers of PTR-MS instruments) results in a lower detection efficiency compared to an *E*/*N* value where the peak intensity is observed (which is humidity dependent). The second practical and more significant implication is that the $TNTH^+$ sensitivity dependence on *E*/*N* can be used to provide a potentially useful discriminatory

analytical procedure for the elimination of false positives with regard to the detection of TNT using PTR-MS technology. This discrimination can be achieved by providing fast switching between *E*/*N* values (e.g. from 180 Td to 110 Td) whilst monitoring the signal intensity at 228 m/z (which is the m/z value corresponding to $TNTH^+$). A drop in intensity would provide a high confidence in assigning an ion observed at 228 m/z to be protonated TNT. Fast switching of *E*/*N* is easily achievable by keeping *N* constant and rapidly changing the voltage applied across the drift tube. If this is combined with the fast switching of reagent ion from for example H_3O^+ to O_2^+, which can occur in seconds, and which results in a change of the product ion, from 228 m/z to 210 m/z, then essentially unambiguous detection of TNT is achieved. Thus, the selectivity for the detection of TNT can be significantly enhanced by the use of a simple automatic computer controlled procedure providing rapid switching of drift tube voltages followed sequentially with a change in the reagent ion. Importantly, the resulting enhanced selectivity for TNT provided by this has important technological applications. Low resolution, smaller and hence low-cost quadrupole mass spectrometers (such as those used in residual gas analysers) could be used in a PTR-MS instrument, rather than the high resolution (and hence expensive) time-of-flight mass spectrometers used in this study. The adoption of cost-efficient mass spectrometers and inclusion of user-friendly feedback to security personnel would result in a rapid and field effective technology that can provide high selectivity and hence a much higher level of confidence for the real-time and rapid analytical detection of TNT than is currently available.

The discovery with TNT has wider implications beyond that of Homeland Security. The observation that drift-tube ion-molecule chemistry can be discriminated by switching bias fields opens a new dimension for proton transfer reaction mass spectrometric techniques. The two-dimensional parameter space offers the potential for unprecedented easy detection capabilities

for specific marker molecules in areas such as food security, breath analysis, atmospheric chemistry, etc. Of course the drift tube reaction pathways have to be understood and suitable markers identified. Nevertheless, we consider this to represent a new field in using PTR-MS techniques for analytical chemistry.

ACKNOWLEDGEMENTS

CAM and PW acknowledge the EPSRC (EP/E027571/1). DBP PhD studentship is funded under the Innovative Research Call in Explosives and Weapons Detection (2010), a cross-government programme sponsored by a number of UK government departments and agencies under the CONTEST strategy. CAM thanks Smiths Detection Ltd for the loan of a KORE PTR-TOF-MS. Work was also partially supported by the Leopold Franzens Universität, Innsbruck, the FWF and FFG, Wien and the European Commission, Brussels. We thank EDA with the JIP-FP programme Contract A-0378-RT GC. FP and SJ acknowledges the support of the Community under a Marie Curie Industry-Academia Partnership and Pathways (Grant Agreement Number 218065).

References

1. Fainberg, A. *Science* **1992**, *255*, 1531-1537.
2. Mäkinen, M.; Nousiainen, M.; Sillanpää, M. *Mass Spectrom. Reviews* **2011**, *30*, 940-973.
3. Eiceman, G. A.; Karpas, Z. *Ion Mobility Spectrometry* 2nd Edition (CRC Press, Boca Raton, 2005).
4. Watts, P. *Anal. Proc.* **1991**, *28*, 328-330.
5. Blake, R. S.; Monks, P. S.; Ellis, A.M. *Chem. Rev.* **2009**, *109*, 861–896.
6. Kirkby, J., et al. *Nature* **2011**, *476*, 429-433.
7. de Gouw, J. A., et al. *Science* **2011**, *331*, (2011)
8. Cordell, R. L.; Wyche, K. P.; Blake, R. S.; Monks, P. S.; Ellis, A. M. *Anal. Chem.* **2007**, *79*, 8359-8366.
1. Mayhew, C. A.; Sulzer, P.; Petersson, F.; Haidacher, S.; Jordan, A.; Märk, L.; Watts P.; Märk, T. D. *Int. J. Mass Spectrom.* **2010**, *289,* 58-63.
2. Petersson, F.; Sulzer, P.; Mayhew, C. A.; Watts, P.; Jordan, A.; Märk L.; Märk. *Rapid Commun. Mass Spectrom.* **2009**, *23*, 3875-3880.
3. Jürschik, S.; Sulzer, P.; Petersson, F.; Mayhew, C. A.; Jordan, A.; Agarwal, B.; Haidacher, S.; Seehauser, H,; Becker, K.; Märk, T. D. *Anal. Bioanal. Chem.* **2010**, *398* 2813-2820.
4. Agarwal, B.; Petersson, F.; Jürschik, S.; Sulzer, P.; Jordan, A.; Märk, T. D.; Watts, P.; Mayhew, C. A. *Anal. Bioanal. Chem*. **2011**, *400*, 2631-2639.
9. DFT calculations were performed using the Gaussian 03 programme with the GaussView interface.(Gaussian 09, Revision A.02, M. J. Frisch, G. W. Trucks, H. B. Schlegel, G. E. Scuseria, M. A. Robb, J. R. Cheeseman, G. Scalmani, V. Barone, B. Mennucci, G. A. Petersson, H. Nakatsuji, M. Caricato, X. Li, H. P. Hratchian, A. F. Izmaylov, J. Bloino, G. Zheng, J. L. Sonnenberg, M. Hada, M. Ehara, K. Toyota, R. Fukuda, J. Hasegawa, M.

Ishida, T. Nakajima, Y. Honda, O. Kitao, H. Nakai, T. Vreven, J. A. Montgomery, Jr., J. E. Peralta, F. Ogliaro, M. Bearpark, J. J. Heyd, E. Brothers, K. N. Kudin, V. N. Staroverov, R. Kobayashi, J. Normand, K. Raghavachari, A. Rendell, J. C. Burant, S. S. Iyengar, J. Tomasi, M. Cossi, N. Rega, J. M. Millam, M. Klene, J. E. Knox, J. B. Cross, V. Bakken, C. Adamo, J. Jaramillo, R. Gomperts, R. E. Stratmann, O. Yazyev, A. J. Austin, R. Cammi, C. Pomelli, J. W. Ochterski, R. L. Martin, K. Morokuma, V. G. Zakrzewski, G. A. Voth, P. Salvador, J. J. Dannenberg, S. Dapprich, A. D. Daniels, O. Farkas, J. B. Foresman, J. V. Ortiz, J. Cioslowski, and D. J. Fox, Gaussian, Inc., Wallingford CT, 2009.)

10. Bell, A. J., Citra, A., Dyke, J. M., Ferrante, F., Gagliardi, L., Watts, P. *PCCP* **2004**, *6*, 1213-1218.

11. http://www.ptrms.com (last accessed February 2012).

12. http://www.kore.co.uk/ (last accessed February 2012).

13. Jordan, A.; Haidacher, S.; Hanel, G.; Hartungen, E.; Märk, L.; Seehauser, H.; Schottkowsky, R.; Sulzer, P.; Märk. T. D. *Int. J. Mass Spectrom*. **2009**, *286*, 122-128.

14. Blake, R. S.; Whyte, C.; Highes, C. O.; Ellis, A. M.; Monks, P. S.; *Anal. Chem.* **2004**, *76*, 3841-3845.

15. Ennis, C. J.; Reynolds, J. C.; Kelyand, B. J.; Carpenter, L. J. *Int. J. Mass Spectrom*. **2005**, *247***,** 72-80.

16. Hansel, A.; Singer, W.; Wisthaler, A.; Schwarzmann, M., Lindinger, W. *Int. J. Mass Spectrom. Ion Processes* **1997**, *167/168*, 697-703.

17. Inomata, S.; Tanimoto, H; Kameyama, S.; Tsunogai, U.; Irie, H.; Kanaya, Y.; Z. Wang**.** *Atmospheric Chemistry and Physics* **2008**, *8*, 273-284.

18. Vlasenko, A.; Macdonald, A.M.; Sjostedt, S. J.; Abbatt, J. P. D. *Atmos. Meas. Tech.* **2010**, *3*, 1055–1062.

19. Christian, T. J. ; Kleiss, B. ; Yokelson, R. J. ; Holzinger, R. ; Crutzen, P. J. ; Hao, W. M. ; Shirai, T. ; Blake, D. R. *J. Geophys. Res.* **2004**, *109*, D02311.

20. Karl, T.; Jobson, T.; Kuster, W. C.; Williams, E.; Stutz, J.; Shetter, R.; Hall, S. R.; Goldan, P.; Fehsenfeld, F.; Lindinger, W. *J. Geophys. Res.* **2003**, *108*, 4508.

21. Knighton, W. B.; Fortner, E. C.; Midey, A. J.; Viggiano, A. A.; Hemdon, S. C.; Wood, E. C.; Kolb, C. E. *International Journal of Mass Spectrometry* **2009**, *283*, 112–121.